The background of the slide is a vibrant, artistic representation of the universe. It features swirling, colorful patterns in shades of teal, orange, and purple, resembling galaxy filaments or nebulae. Scattered throughout are numerous small, bright yellow and white stars, along with larger, glowing spheres in various colors like orange, blue, and purple, which could represent distant galaxies or celestial bodies. The overall effect is a rich, multi-colored cosmic scene.

Growth history and quasar bias evolution at $z < 3$ from Quaia

Giulia Piccirilli (Univ. Torino)

JCAP 06(2024)012

with

*G. Fabbian, D. Alonso, K. Storey-Fisher, C. Garcia-Garcia, J. Carron and A.
Lewis*

Overview

We use the clustering of Quiaia quasars and their cross-correlation with CMB lensing maps to achieve three main goals

- ① Measurement of σ_8 as function of z at high redshift ($z \sim 3$)
- ② Study of the bias of quasars
- ③ Investigate the presence of possible systematics in CMB lensing reconstructions

Cross-correlation framework

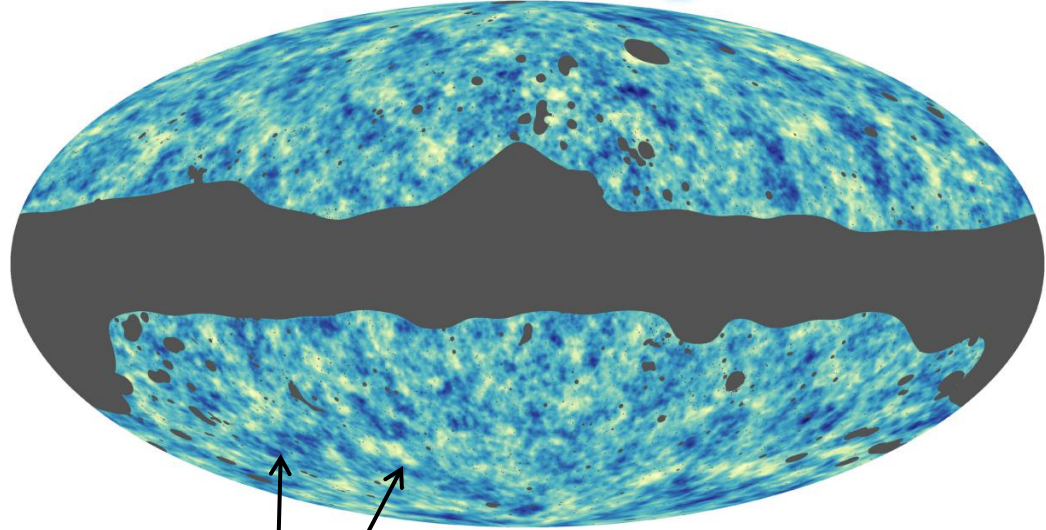
Why are we interested in cross-correlation analysis

This is an invaluable tool for **probing the Universe** and **maximizing** the extraction of **information** from diverse datasets:

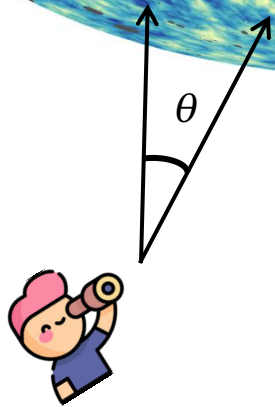
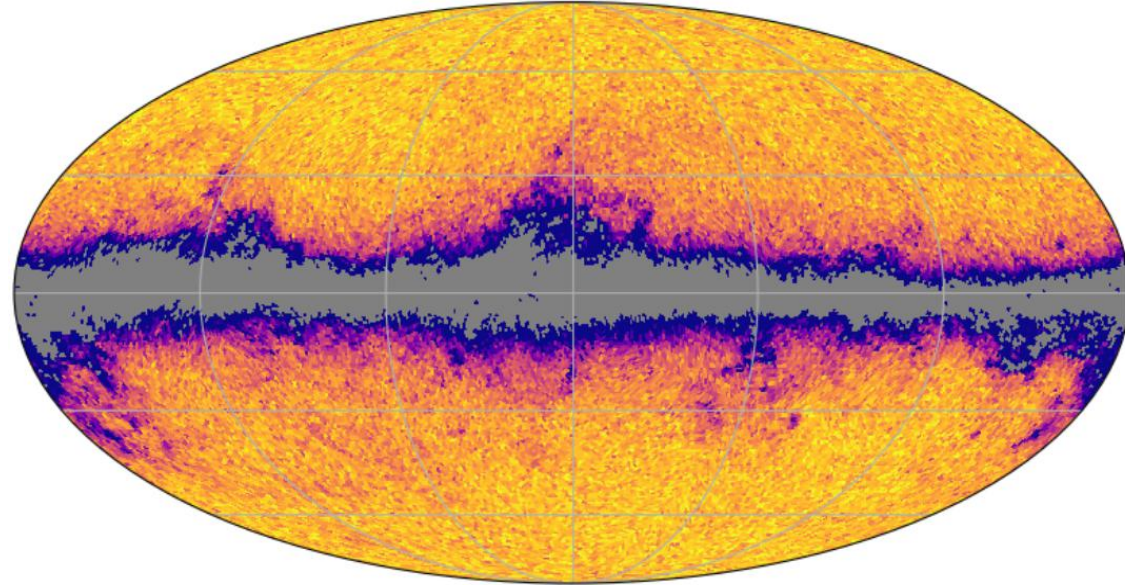
- ① enhanced control over systematic effects compared to auto-correlation analyses
- ② constraining cosmological and nuisance parameters
- ③ revealing signals otherwise hidden by the noise level (e.g. Integrated Sachs Wolfe, ISW effect)

Cross-correlation: statistical tools

CMB lensing



LSS survey: Quiaia



angular 2-point correlation function

angular power spectrum

$$C(\theta) = \sum_{\ell=0}^{\infty} \left(\frac{2\ell + 1}{4\pi} \right) C_{\ell} P_{\ell}(\cos \theta)$$

$$C_{\ell} = \frac{1}{2\ell + 1} \sum_{m=-\ell}^{\ell} \langle |a_{\ell m}|^2 \rangle$$

Cross-correlation: statistical tools

Auto angular power spectrum of quasars

$$C_{\ell}^{g g} = \frac{2}{\Pi} \int_0^{\infty} dz [W^g(z)]^2 \int_0^{\infty} dk k^2 P(k, z) j_{\ell}^2[k \chi(z)]$$

Cross angular power spectrum

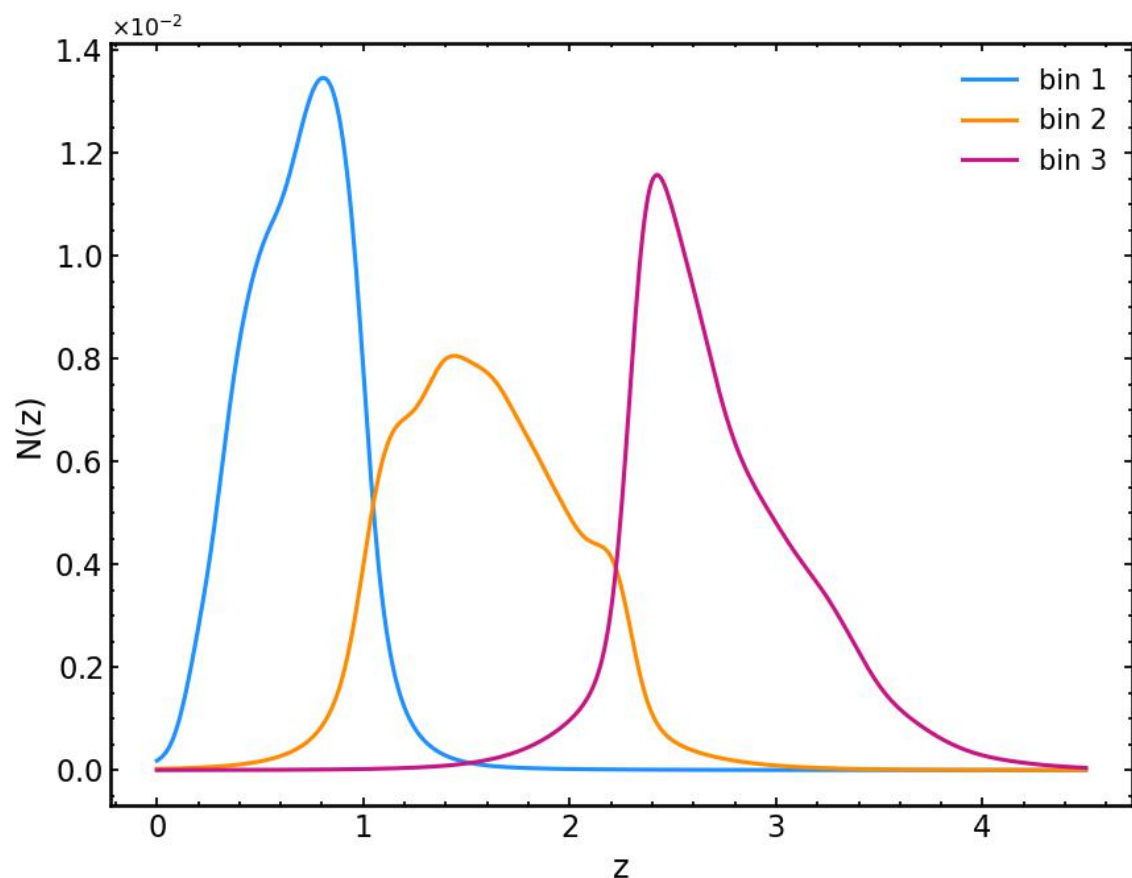
$$C_{\ell}^{\kappa g} = \frac{2}{\Pi} \int_0^{\infty} dz W^g(z) \int_0^{\infty} dz' W^{\kappa}(z') \times \int_0^{\infty} dk k^2 P(k, z, z') j_{\ell}[k \chi(z)] j_{\ell}[k \chi(z')]$$

g window function: $W^g(z) = \frac{b(z)N(z)}{\int dz' N(z')}$

κ window function: $W^{\kappa}(z) \propto \frac{(1+z)\chi(z)}{H(z)} \frac{\chi^* - \chi(z)}{\chi^*}$

Datasets: the Quiaia catalogue

Gaia-unWise quasar catalog is an all sky survey with median redshift $z = 1.67$ and with 1,295,502 sources brighter than the limiting magnitude $G=20.5$ (*K. Storey-Fisher +, 2023*)



The measured bias in the redshift bins is well described by (*P. Laurent +, 2017*)

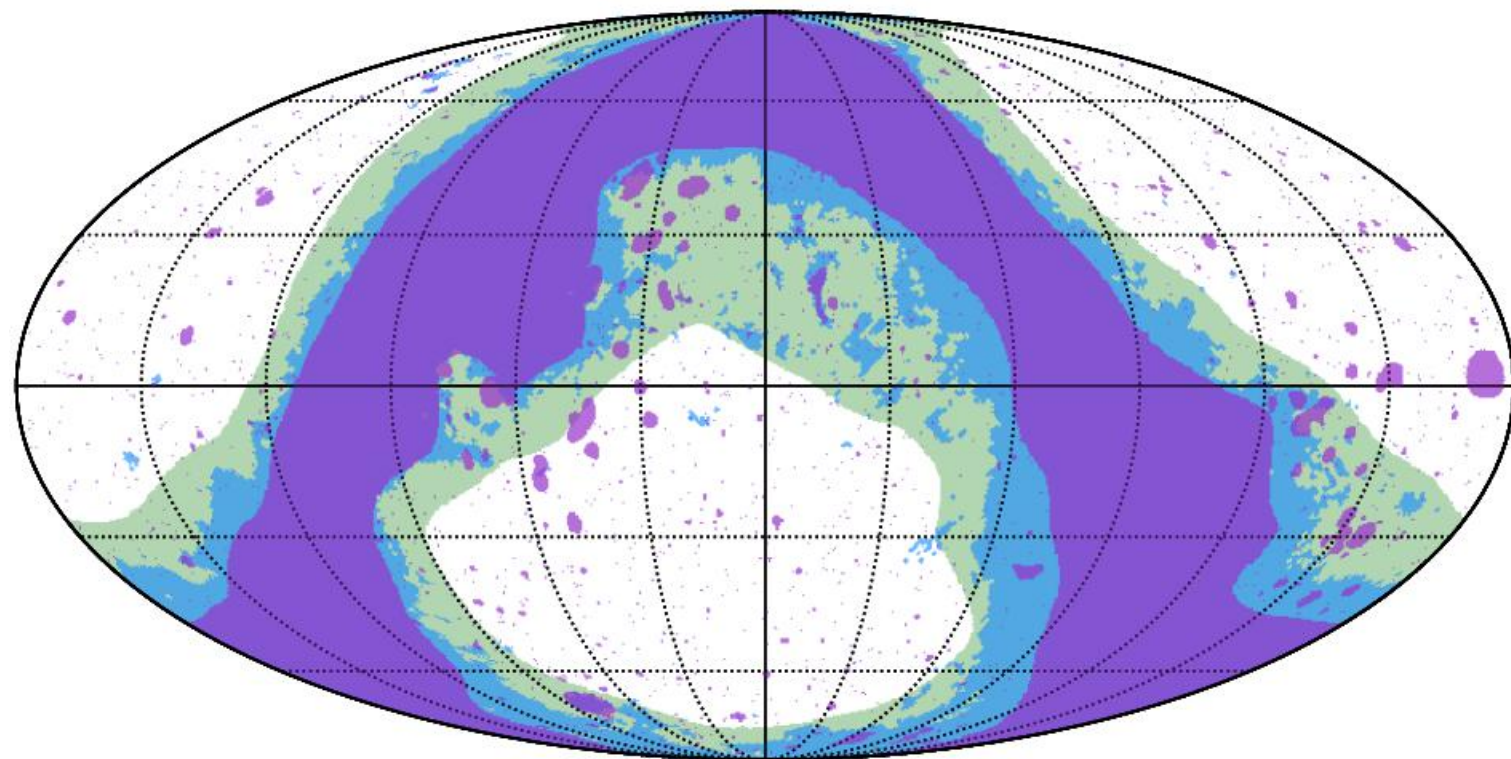
$$b^i(z) = b_g^i [0.278 (1 + z)^2 + \text{const}]$$

Datasets: CMB lensing maps

All maps are based on the latest Planck data release (PR4) but are obtained using different combinations of temperature and polarization data

Baseline

- ① Generalized Minimum-Variance (“GMV”)
- ② No-temperature (“No-TT”)
- ③ Polarisation-only (“Pol-only”)
- ④ Temperature alone (“TT-only”)
- ⑤ SZ-deprojected (“TT-noSZ”)

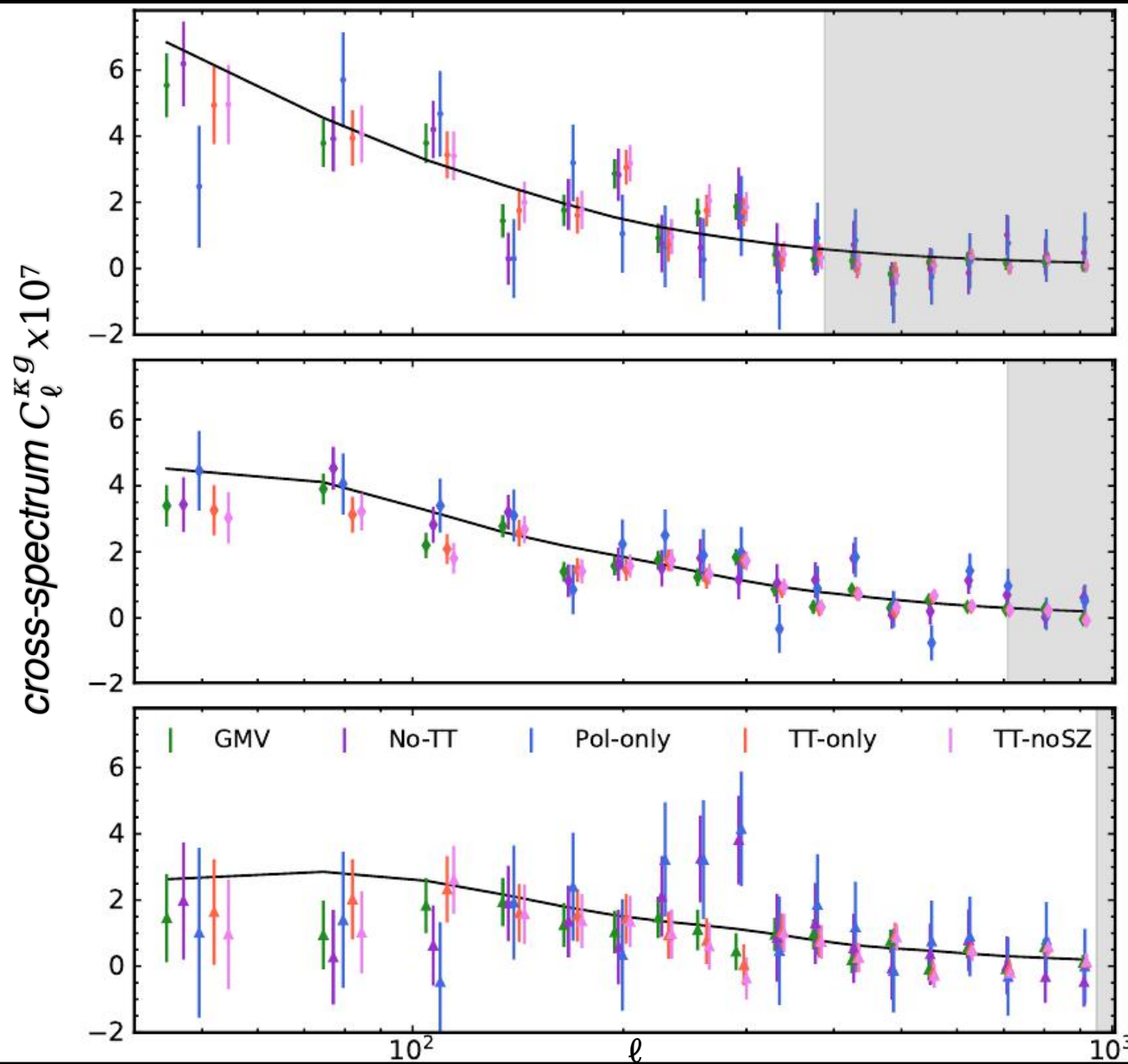
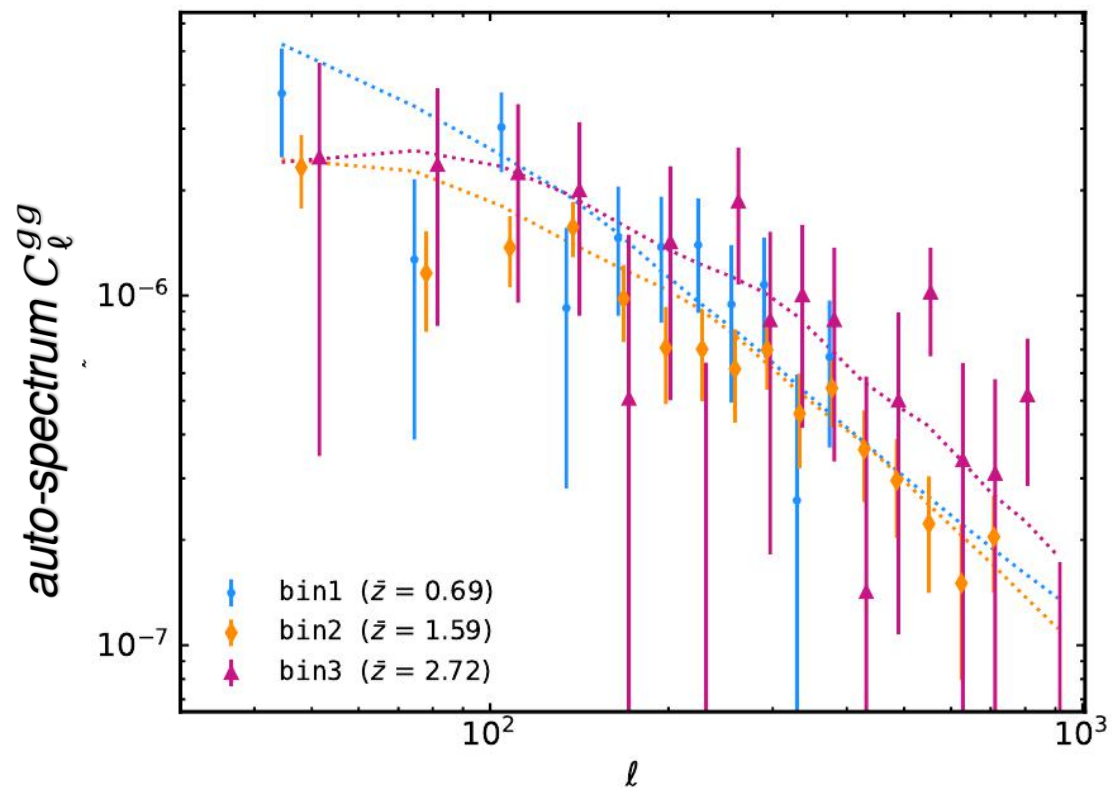


CMB lensing

Quia

Planck Galactic Mask

Measured power spectra



Detection significance

$$S/N \equiv \sqrt{\chi_{null}^2 - \chi^{bf}}$$

	C_{ℓ}^{gg}	$C_{\ell}^{kg, No-TT}$	$C_{\ell}^{kg, GMV}$	$C_{\ell}^{kg, Pol-only}$	$C_{\ell}^{kg, TT-only}$	$C_{\ell}^{kg, no-SZ}$
bin1	7.5	8.7	13.5	5.4	11.1	11.4
bin2	14.7	13.5	20.0	10.0	15.5	15.1
bin3	5.9	5.1	5.7	2.9	5.0	3.8
All	17.3	16.2	24.7	11.6	19.8	19.4

Detection significance

$$S/N \equiv \sqrt{\chi_{\text{null}}^2 - \chi^{\text{bf}}}$$

	C_{ℓ}^{gg}	$C_{\ell}^{\kappa g, \text{No-TT}}$	$C_{\ell}^{\kappa g, \text{GMV}}$	$C_{\ell}^{\kappa g, \text{Pol-only}}$	$C_{\ell}^{\kappa g, \text{TT-only}}$	$C_{\ell}^{\kappa g, \text{no-SZ}}$
bin1	7.5	8.7	13.5	5.4	11.1	11.4
bin2	14.7	13.5	20.0	10.0	15.5	15.1
bin3	5.9	5.1	5.7	2.9	5.0	3.8
All	17.3	16.2	24.7	11.6	19.8	19.4

baseline CMB lensing maps

Likelihood analysis

Gaussian Likelihood using $C_\ell^{Kg} + C_\ell^{gg}$ as dataset to constrain simultaneously σ_8 and the QSO bias (Core Cosmology Library + Cobaya)

Explored cosmological models:

- ① CosmoFix: cosmological parameters fixed to Planck2020 best-fit values. Free parameters $\{b_g^i\}$
- ② CosmoMarg: $\{\Omega_M, \sigma_8, h, b_g^i\}$
- ③ CosmoGrowth: $\{\Omega_M, h, \Delta_i, b_g^i\}$

Likelihood analysis

Gaussian Likelihood using $C_{\ell}^{kg} + C_{\ell}^{gg}$ as dataset to constrain simultaneously σ_8 and the QSO bias (Core Cosmology Library + Cobaya)

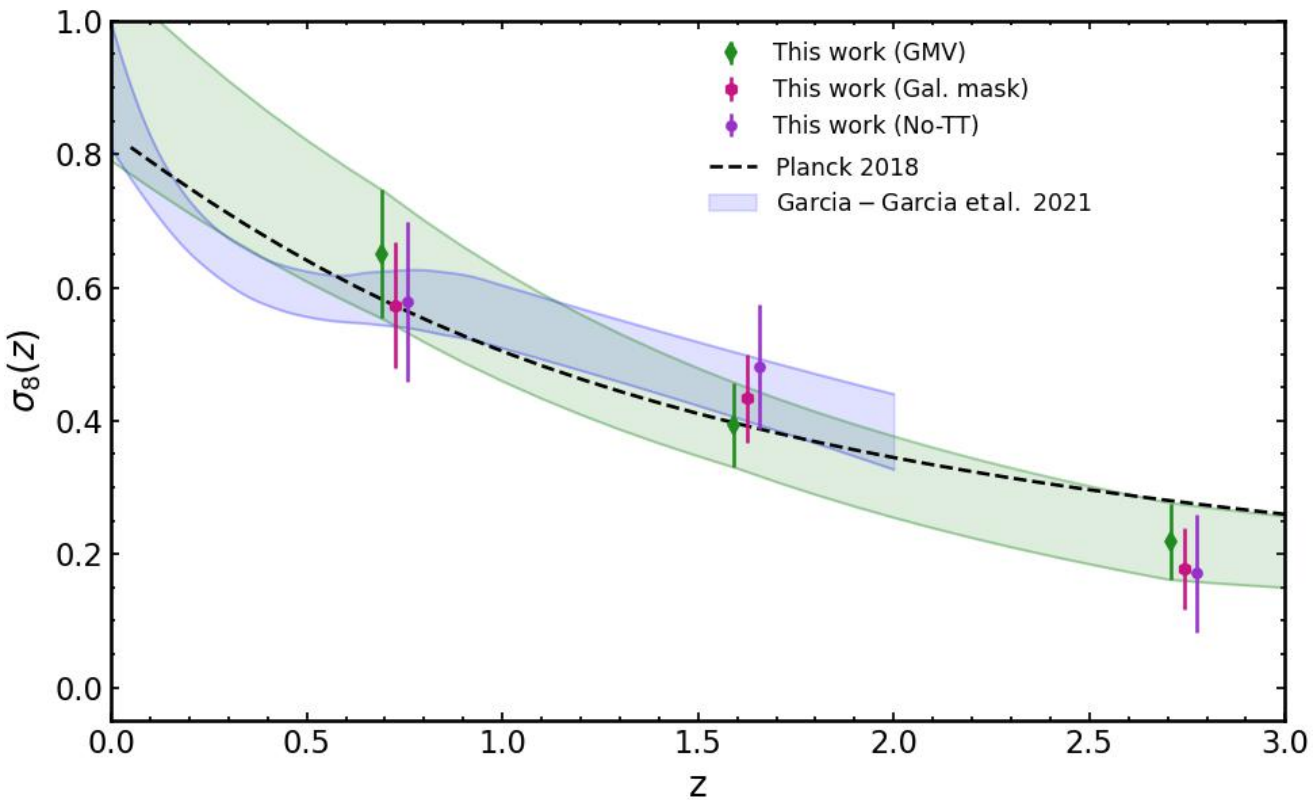
Explored cosmological models:

- 1 CosmoFix: cosmological parameters fixed to Planck2020 best-fit values. Free parameters $\{b_g^i\}$
- 2 CosmoMarg: $\{\Omega_M, \sigma_8, h, b_g^i\}$
- 3 CosmoGrowth: $\{\Omega_M, h, \Delta_i, b_g^i\}$

$$P_{lin}(k, z) = \mathbf{D}(z)^2 P_{lin}(k, z = 0)$$

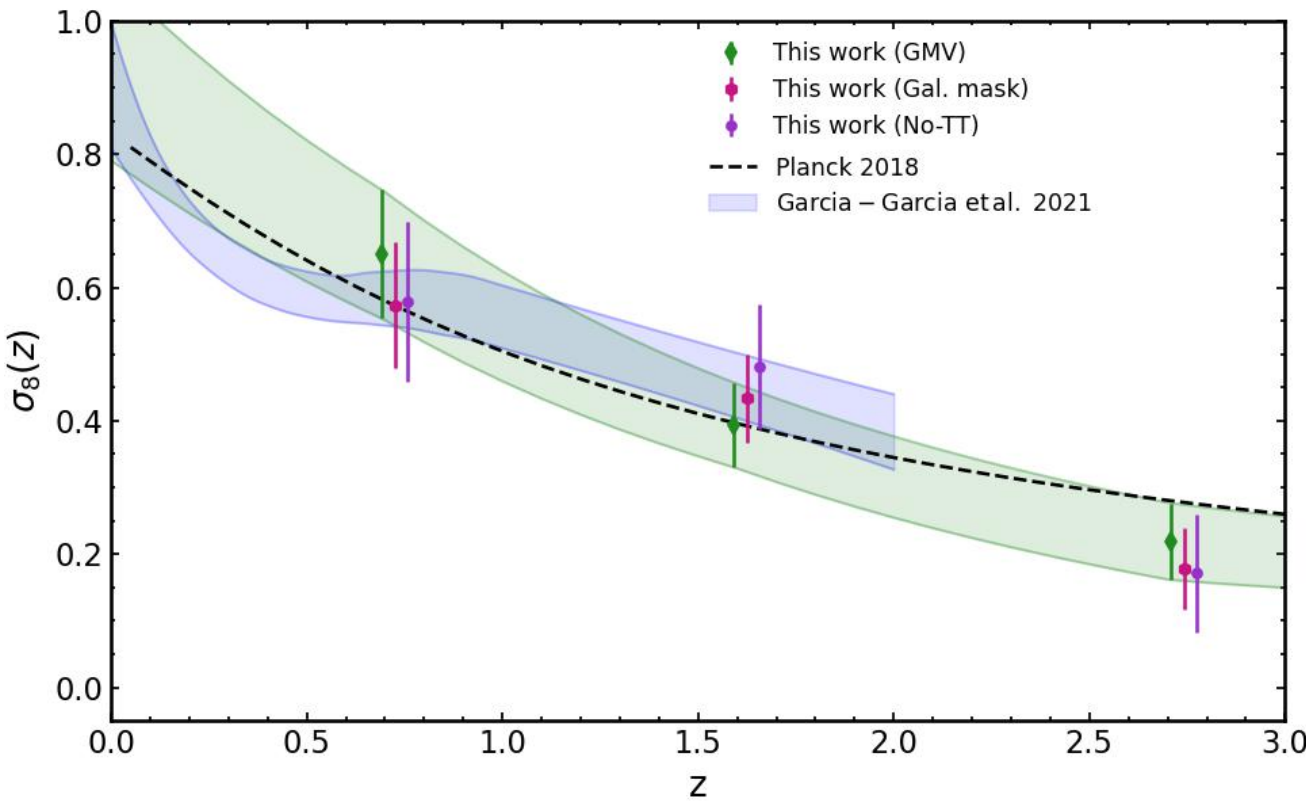
$$\sigma_8 = \sigma_{8,\text{fid}} \mathbf{D}(z)^{\text{fid}} (1 + \Delta_i)$$

Results 1: Measurements of σ_8

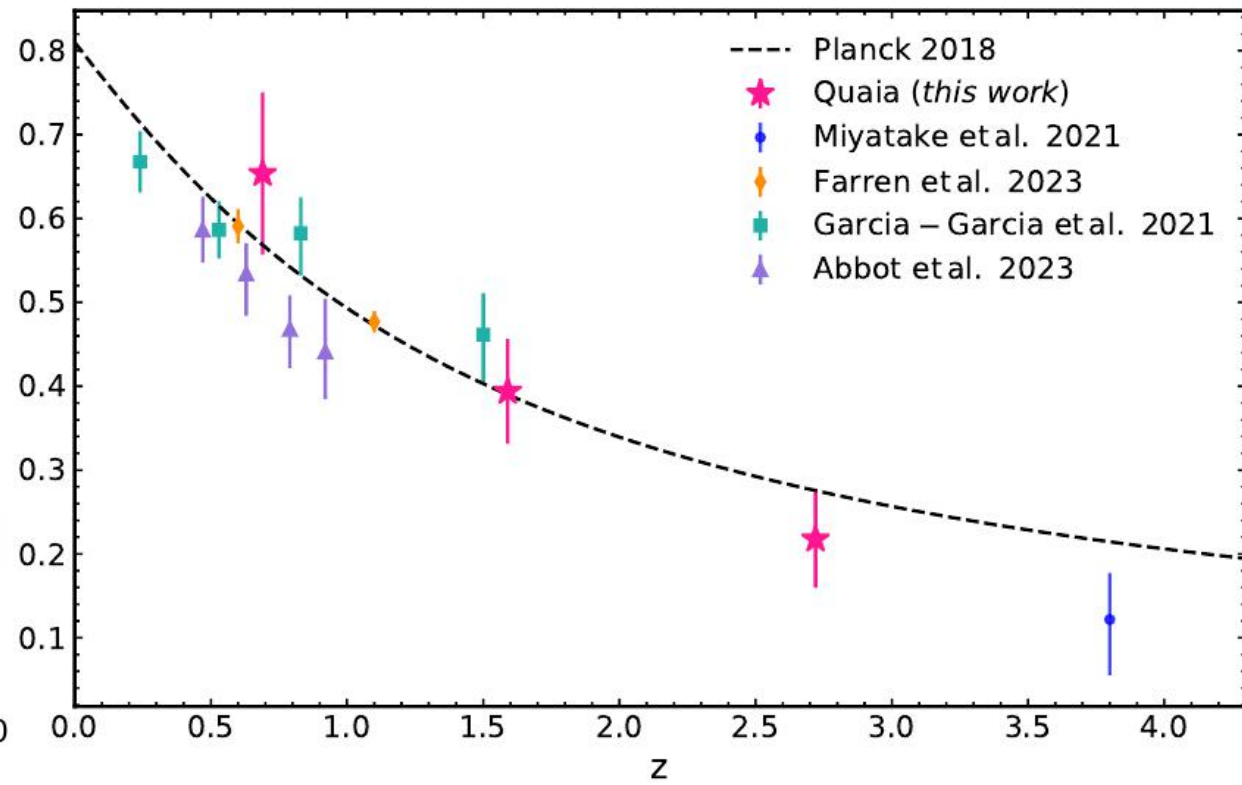


Our results are in agreement (within $\sim 1\sigma$) with Λ CDM prediction using Planck2020 best-fit parameters

Results 1: Measurements of σ_8

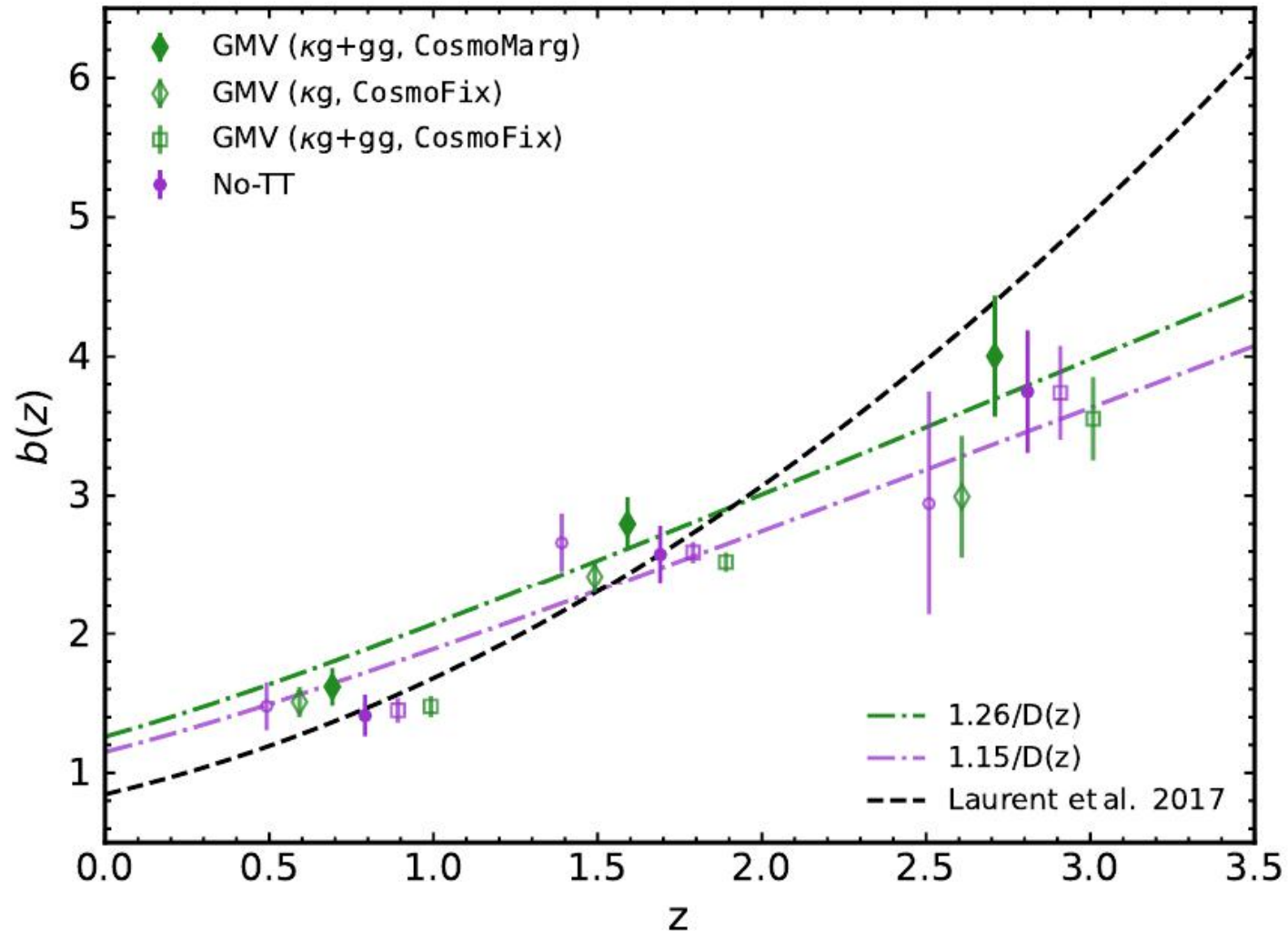


Our results are in agreement (within $\sim 1\sigma$) with Λ CDM prediction using Planck2020 best-fit parameters



One of the highest measurement in redshift of $\sigma_8(z)$!

Results 2: Quasar bias



General good agreement with *Laurent+, 2017*

Milder evolution at higher redshifts more compatible with: $b(z) = b_0/D_{\text{fid}}(z)$

Results are not strongly driven by contamination from extragalactic foregrounds in the CMB lensing map.

Results 3: study of contaminations in CMB maps

D. Alonso +, 2023 reported a potentially significant difference in the amplitude of the Quiaia-CMB lensing cross-correlation using different κ maps at high redshifts

Isolating the range of redshifts is interesting to establish its potential extragalactic origin

Set up:

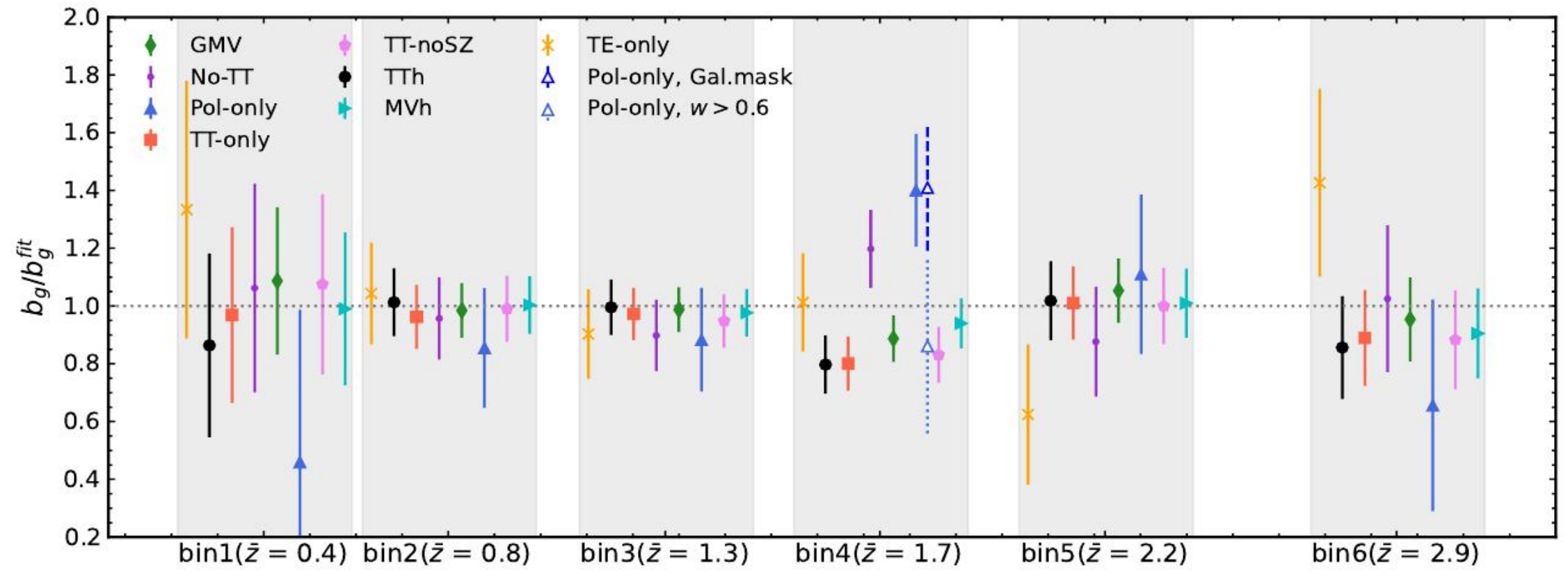
- ① We divide the total redshift distribution of the Quiaia sources into six redshift bins ($z_{edges} = [0.0, 0.5, 1.0, 1.5, 2.0, 2.5, 5]$)
- ② CosmoFix cosmological model
- ③ More CMB lensing maps: TE-only (“TE-only”), Minimum-variance source hardened (“MVh”), Temperature-only, source-hardened map (“TTh”)

Results 3: study of contaminations in CMB maps

$$b_g = \frac{t^T \text{Cov}^{-1} d}{t^T \text{Cov}^{-1} t} \quad \sigma(b_g) = \frac{1}{\sqrt{t^T \text{Cov}^{-1} t}}$$

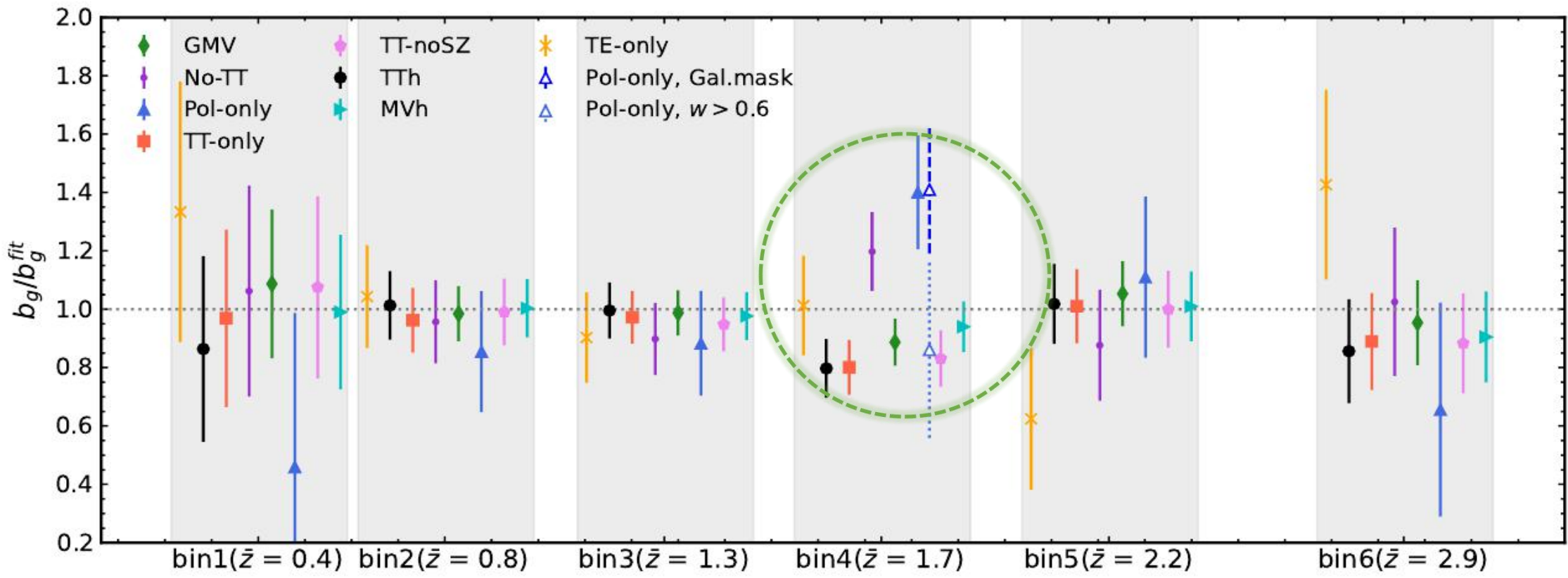
Results 3: study of contaminations in CMB maps

$$b_g = \frac{t^T Cov^{-1} d}{t^T Cov^{-1} t} \quad \sigma(b_g) = \frac{1}{\sqrt{t^T Cov^{-1} t}}$$



Results 3: study of contaminations in CMB maps

$$b_g = \frac{t^T Cov^{-1} d}{t^T Cov^{-1} t} \quad \sigma(b_g) = \frac{1}{\sqrt{t^T Cov^{-1} t}}$$



Conclusions

- ① One of the highest-redshift constraints on σ_8 in the literature ($\sigma_8(z = 2.7) = 0.22 \pm 0.06$)
- ② The $b(z)$ is overall comparable to that of eBOSS with a milder evolution at high redshifts. We find a dependency on the choice of cosmological model but our results are largely compatible between different analysis choices.
- ③ We investigated the presence of foreground contamination in the Planck lensing maps, finding a localized effect at $z \sim 1.7$ which can be explained by the extragalactic contamination from a clustered component. Nevertheless, we verified that our constraints on $\sigma_8(z)$ are not significantly affected by this potential systematic.

NEXT STEP: Use new CMB experiments (ACT, SO, and CMB Stage-4) that will probe significantly smaller angular scales with higher sensitivity, and over a wide range of frequencies, making it possible to improve the robustness of these constraints to both Galactic and extragalactic systematics.

The background is a vibrant, abstract space-themed illustration. It features flowing, wavy bands of color in shades of teal, green, yellow, orange, and purple, set against a dark, starry background. Several bright orange spheres are scattered throughout the scene. In the bottom left corner, the back of a person's head is visible, showing curly orange hair and a white garment with a black collar. A semi-transparent purple rectangular box is centered horizontally across the middle of the image, containing the text "Thanks :)".

Thanks :)

Results 3: Statistical significance

Lensing maps

We retrieved the κ maps using 480 independent realizations of simulated lensing reconstructions (PR4)

1

2

b_g estimates

We computed the cross-spectrum for each realization and reconstruction method, and estimated the value of b_g

3

4

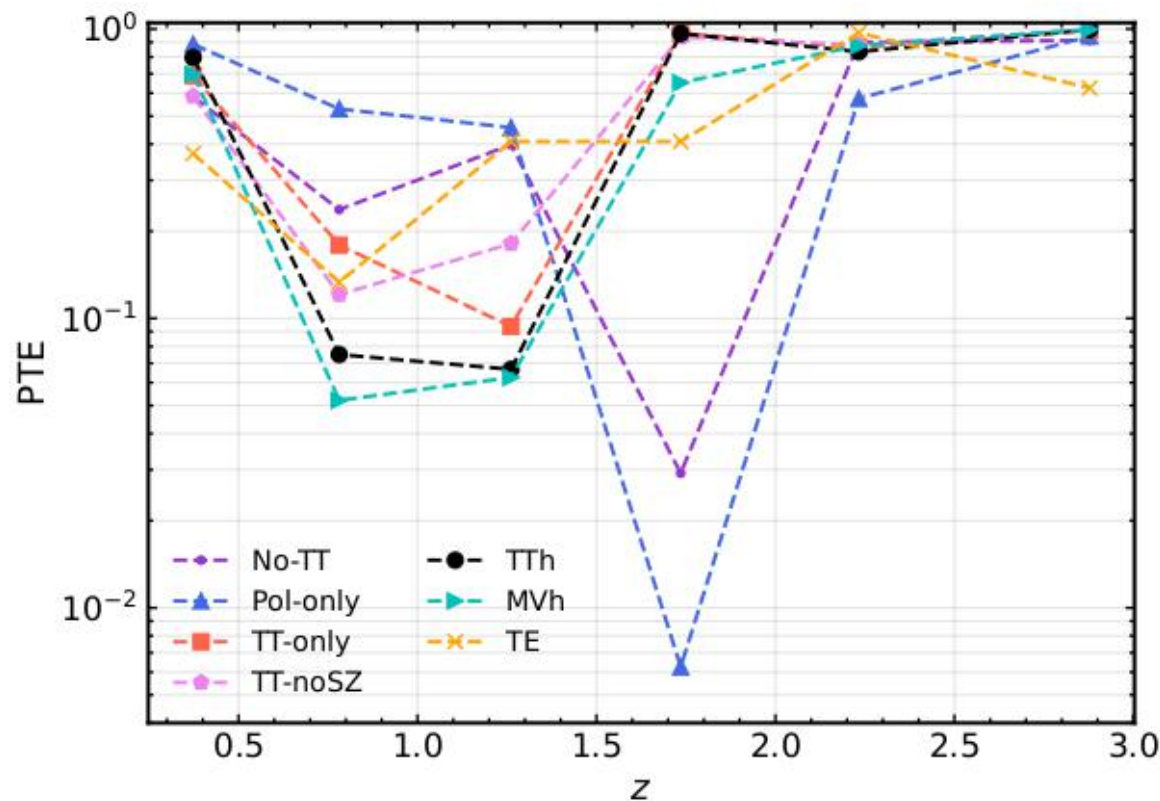
Correlated Gaussian realizations

We generated a correlated Gaussian realization of the QSOs overdensity map. We assumed the theoretical auto and cross-correlation, the same cosmology as in PR4 simulations, and the fiducial $b(z)$ and $N(z)$.

We added a shot noise component modeled using random realizations from the Quia catalog

PTE

We quantify the level of disagreement between different CMB lensing maps by calculating the fraction of simulated realizations for which a difference in the value of b_g with respect to the one found for the corresponding GMV map is larger than the value measured in the data.



Quaia: old vs new catalogue

